

Phonon Quantum Nondemolition Measurements in Nonlinearly Coupled Optomechanical Cavities

B.D. Hauer,^{1,*} A. Metelmann,² and J.P. Davis^{1,†}

¹*Department of Physics, University of Alberta, Edmonton, Alberta, Canada T6G 2E9*

²*Dahlem Center for Complex Quantum Systems and Fachbereich Physik, Freie Universität Berlin, 14195 Berlin, Germany*

(Dated: July 23, 2022)

In the field of cavity optomechanics, proposals for quantum nondemolition (QND) measurements of phonon number provide a promising avenue by which one could study the quantum nature of nanoscale mechanical resonators. Here, we investigate these QND measurements for an optomechanical system whereby quadratic coupling arises due to shared symmetries between a single optical and mechanical mode. We establish a relaxed limit on the amount of linear coupling that can exist in this type of system while still allowing for a QND measurement of Fock states. With this new condition, optomechanical QND measurements could be used to probe the decoherence of mesoscopic mechanical Fock states, providing an experimental testbed for quantum collapse theories.

The theory of quantum mechanics has excelled in describing a multitude of phenomena associated with microscopic systems. However, as a system scales to larger sizes, interaction with the surrounding environment causes its quantum mechanical state to decohere into the classical realm [1, 2]. Although there are a number of theories proposing mechanisms by which such decoherence could occur [3–6], this quantum-to-classical transition is poorly understood, largely due to a lack of experimental systems that can be used to study these processes. To this end, a number of proposals have been put forward to use cavity optomechanics as an experimental platform to fill this void [7–10].

In cavity optomechanics, confined photonic degrees of freedom interact via radiation pressure with a mechanical resonator [20], allowing one to prepare the mechanical element into a variety of quantum states [13–18]. Though experimental progress in quantum cavity optomechanics has been astounding [9, 14, 18, 20–28, 30–33], a vital experiment still remains: the quantum nondemolition (QND) measurement of the phononic Fock states of a mechanical resonator [14, 18]. While QND measurements have been demonstrated for single particles [34, 35], photons [36, 37], spins [38], and superconducting qubits [39], as well as for a single quadrature of a micromechanical resonator [27, 28], measurements of the mechanical Fock states of a cavity optomechanical system would provide an engineerable platform to directly probe the decoherence of a mesoscopic quantum state. However, performing an experiment of this nature proves to be difficult, largely due to the fact that most conventional optomechanical cavities couple linearly to the position of the mechanical resonator [20]. Such a measurement scheme is unsuitable for QND measurement of the resonator’s quantized energy [40], as it is subject to the Heisenberg uncertainty principle, resulting in the standard quantum limit on how precisely the system can be monitored continuously [19, 41, 42]. One must then turn to an optomechanical system where the optical mode is directly coupled to the square of the mechanical position, providing a method by which QND measurements of the phonon

number states of the system can be performed [14, 18].

Experimental demonstration of quadratic coupling in optomechanical systems has been largely focussed on membrane-in-the-middle (MIM) systems (see Fig. 1a), whereby a mechanical element – which is typically a thin dielectric membrane [1, 18, 45], but can also be a cloud of cold atoms [46] or a photonic crystal nanobeam [3, 7] – is placed within an optical cavity. Inserting the “membrane” causes the degenerate optical modes of the cavity to hybridize into two supermodes that exhibit an avoided level crossing mediated by photon tunneling through the mechanical element [1, 3]. By moving the membrane to an antinode of the optical mode, linear coupling of the membrane’s motion is suppressed and quadratic coupling becomes dominant [1, 3, 18]. However, when optically driving one of these supermodes, parasitic linear coupling to the membrane’s position emerges in the opposite mode, leading to an accelerated decoherence of the membrane’s Fock state that can only be overcome in the single-photon strong-coupling regime [2, 5, 6]. This stringent constraint has proven to be the most difficult obstacle to performing QND measurements of phonon number in a MIM optomechanical system [3].

In this paper, we consider an optomechanical system which exhibits second-order coupling due to the shared symmetries between the mechanical resonance and a single optical mode [13]. Such a system could be physically realized as an out-of-plane flexural (or torsional) mode of a mechanical resonator side-coupled to a whispering gallery mode (WGM) of a microdisk [8] (see Fig. 1b) or the in-plane motion of a paddle located within a photonic crystal nanobeam [13]. Here, we analyze this type of quadratically-coupled optomechanical system and arrive at the relevant requirements associated with resolving the thermally-induced quantized jumps between the energy eigenstates of the mechanical resonator. In doing so, we derive a limit that places a constraint on the relative strengths of the linear and quadratic optomechanical coupling of the system. Furthermore, we show that in the case of a MIM system, this generalized limit is equivalent to the single-photon strong-coupling regime. The ability to perform these types of QND measurements would provide a direct probe of the quantum decoherence of a mesoscopic quantum state, furthering our understanding of the mechanisms by which quan-

*Electronic address: bhauer@ualberta.ca

†Electronic address: jdavis@ualberta.ca

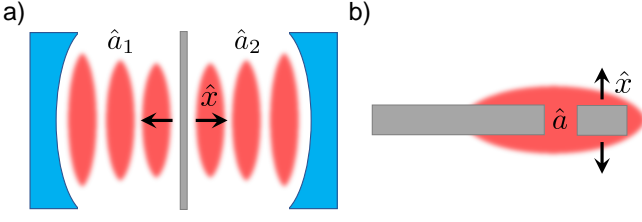


FIG. 1: Schematic of a) a membrane-in-the-middle optomechanical system and b) a mechanical element side-coupled to a whispering gallery mode optical cavity. In a), quadratic coupling arises due to an avoided crossing between the two optical modes, labeled by their creation operators \hat{a}_1 and \hat{a}_2 . Meanwhile, in b), the single optical mode denoted by \hat{a} is coupled to the square of the mechanical motion via shared symmetries between the optics and mechanics. In each of a) and b), the direction of the mechanical displacement, \hat{x} , is indicated by the black arrows.

tum systems transition into the classical regime.

We begin by modeling this optomechanical system as two quantum harmonic oscillators, one that describes the optical cavity, the other the mechanical resonator, leading to the Hamiltonian

$$\hat{H} = \hbar\omega_c(\hat{x})\hat{a}^\dagger\hat{a} + \hbar\omega_m\hat{b}^\dagger\hat{b}. \quad (1)$$

Here \hat{a} and \hat{b} (\hat{a}^\dagger and \hat{b}^\dagger) are the annihilation (creation) operators of the optical cavity and the mechanical resonator, each with an angular resonant frequency of $\omega_c(\hat{x})$ and ω_m . Coupling between the two oscillators arises due to the fact that the resonant frequency of the optical cavity is dependent on the position operator of the mechanics, $\hat{x} = x_{\text{zpf}}(\hat{b} + \hat{b}^\dagger)$, where we have introduced the zero-point fluctuation amplitude $x_{\text{zpf}} = \sqrt{\hbar/2m\omega_m}$, with m being the effective mass of the mechanical oscillator [54]. Expanding the position-dependence of the cavity frequency to second order in \hat{x} , we obtain

$$\omega_c(\hat{x}) = \omega_c + G_1\hat{x} + \frac{G_2}{2}\hat{x}^2, \quad (2)$$

where ω_c is the unperturbed cavity frequency, along with the first- and second-order optomechanical coupling coefficients $G_1 = d\omega_c/d\hat{x}$ and $G_2 = d^2\omega_c/d\hat{x}^2$. Inputting our expansion for $\omega_c(\hat{x})$, as well as our expression for \hat{x} in terms of \hat{b} and \hat{b}^\dagger , into the above Hamiltonian results in

$$\hat{H} = \hat{H}_0 + \hat{H}', \quad (3a)$$

$$\hat{H}_0 = \hbar \left[\omega_c + g_2 \left(\hat{b}^\dagger\hat{b} + \frac{1}{2} \right) \right] \hat{a}^\dagger\hat{a} + \hbar\omega_m\hat{b}^\dagger\hat{b}, \quad (3b)$$

$$\hat{H}' = \hbar g_1 (\hat{b} + \hat{b}^\dagger) \hat{a}^\dagger\hat{a} + \frac{\hbar g_2}{2} (\hat{b}\hat{b} + \hat{b}^\dagger\hat{b}^\dagger) \hat{a}^\dagger\hat{a}, \quad (3c)$$

where we have introduced the single photon, single (two) phonon coupling rate $g_1 = G_1 x_{\text{zpf}}$ ($g_2 = G_2 x_{\text{zpf}}^2$).

We have chosen to separate \hat{H} into two sub-Hamiltonians, \hat{H}_0 and \hat{H}' , such that \hat{H}_0 commutes with the phonon number operator of the mechanical resonator, $\hat{n} = \hat{b}^\dagger\hat{b}$, while \hat{H}' does

not. In this way, \hat{H}_0 represents a QND measurement of the mechanical energy of the resonator [41, 42], whereby changes in phonon number – whether induced thermally or via optomechanical interaction – reflect a per phonon shift of g_2 in the optical cavity’s resonant frequency. We note that even in the zero-temperature limit where no phonons occupy the mechanical resonator, there still exists a static shift of $g_2/2$ in the optical cavity’s resonant frequency corresponding to the mechanical ground state motion, although this static shift is very difficult to measure experimentally [1]. On the other hand, $[\hat{H}', \hat{n}] \neq 0$ such that \hat{H}' , which contains the interaction terms that process in time, acts to contaminate the QND measurement. This is a well-known fact for the first term in \hat{H}' , whereby linear coupling simultaneously probes the phase and energy of the mechanical resonator, preventing a QND Fock state measurement [1, 40]. In principle, one could completely eliminate this linear coupling by properly tuning the optical and mechanical symmetries of the system (see Supplementary Information). However, for any realistic optomechanical cavity, a non-zero amount of linear coupling will always creep into the system due to experimental inaccuracies [8, 13, 18]. Therefore, we seek to set a limit on the maximum allowable linear coupling strength that can exist in a quadratically-coupled optomechanical device that one wishes to use for a QND measurement of phonon number. Furthermore, we look to determine the optomechanical regime for which the second term in \hat{H}' can be safely ignored. As we will see below, this corresponds to the optomechanical equivalent of the rotating wave approximation [20], for which one averages out rapidly oscillating terms in the Hamiltonian in favor of those constant in time. In order to determine these limits, we will apply \hat{H}' as a perturbation to the QND Hamiltonian, \hat{H}_0 , and examine the rates at which these linear and quadratic measurements cause the resonator to transition from a given Fock state. Comparing these two rates to the mechanical resonator’s intrinsic thermal decoherence rate and the optomechanical phonon state measurement rate, we determine a regime where QND measurements of phonon number can be achieved.

We start by determining the intrinsic thermal decoherence rate of the mechanical resonator’s phononic number states. If the mechanical resonator is initialized to its n th Fock state, interactions with a thermal bath at a temperature T will cause this state to decohere at a rate that is determined to be (see Supplementary Information)

$$\Gamma_{\text{th}} = \Gamma_m [(\bar{n}_{\text{th}} + 1)n + \bar{n}_{\text{th}}(n + 1)], \quad (4)$$

where $\bar{n}_{\text{th}} = (e^{\hbar\omega_m/k_B T} - 1)^{-1}$ is the average thermal occupation number of the bath according to Bose-Einstein statistics, evaluated at the mechanical resonance frequency, while Γ_m is the system’s intrinsic mechanical damping rate [1, 14, 21, 22]. We note that this decoherence rate decreases as we move to lower Fock states, taking on its minimum value in the quantum ground state (see Fig. 2). Furthermore, this rate can be decreased by reducing the thermal occupation of the bath as low as possible.

In order to temporally resolve jumps between the mechanical resonator’s phonon number states, one must measure the

system faster than this thermally-induced decoherence rate. It was shown in Ref. [14] that for QND measurements of phonon number associated with \hat{H}_0 , the measurement rate will be given by

$$\Gamma_{\text{meas}} = \bar{C}_2 \Gamma_{\text{m}}. \quad (5)$$

Here, $\bar{C}_2 = \bar{N}C_2$ is the second-order, cavity-enhanced cooperativity of the system, given in terms of the second-order, single-photon cooperativity $C_2 = 4g_2^2/\kappa\Gamma_{\text{m}}$, where κ and \bar{N} are the decay rate and average photon occupation of the optical cavity [20].

Unfortunately, QND measurements of this form will also be contaminated by measurement-induced transitions from $n \rightarrow n \pm 1$ and $n \rightarrow n \pm 2$ due to the first and second terms in \hat{H}' , respectively. The transition rates associated with these processes are determined to be (see Supplementary Information)

$$\begin{aligned} \Gamma_{n+1} &= (n+1)g_1^2 S_{NN}(-\omega_{\text{m}}), \\ \Gamma_{n-1} &= ng_1^2 S_{NN}(\omega_{\text{m}}), \\ \Gamma_{n+2} &= (n+1)(n+2)\frac{g_2^2}{4} S_{NN}(-2\omega_{\text{m}}), \\ \Gamma_{n-2} &= n(n-1)\frac{g_2^2}{4} S_{NN}(2\omega_{\text{m}}), \end{aligned} \quad (6)$$

where we have introduced the spectral density of the photon cavity number, $S_{NN}(\omega)$, given by [17, 19]

$$S_{NN}(\omega) = \frac{\bar{N}\kappa}{(\omega - \Delta)^2 + (\kappa/2)^2}. \quad (7)$$

Here $\Delta = \omega_{\text{c}} - \omega_{\text{d}} + g_2(\bar{n} + \frac{1}{2})$ is the detuning of the drive laser's frequency, ω_{d} , from the cavity resonance, which is shifted in proportion to the average phonon occupancy of the mechanical resonator, $\bar{n} = \langle \hat{n} \rangle$.

Using the rates found in Eqs. (S40-S39), one finds the following hierarchy of rates required to perform optomechanical QND measurements of mechanical energy quantization

$$\Gamma_{\text{meas}} \gg \Gamma_{\text{th}} \gg \Gamma_{n\pm 1}, \Gamma_{n\pm 2}. \quad (8)$$

The right hand side of Eq. (8) ensures that thermal transitions dominate over the optically-induced phonon jumps present due to the measurement itself, leading to the ‘‘linear-coupling condition’’, $\Gamma_{\text{th}} \gg \Gamma_{n\pm 1}$, and the ‘‘quadratic-coupling condition’’, $\Gamma_{\text{th}} \gg \Gamma_{n\pm 2}$. Furthermore, we have the ‘‘fast-measurement condition’’ $\Gamma_{\text{meas}} \gg \Gamma_{\text{th}}$ [14], which tells us that one must be able to measure the phonon state of the resonator before it thermally decoheres in order to resolve quantized mechanical energy jumps [1, 6, 16, 18]. Using this condition, we can determine the largest Fock state number that can be continuously monitored using this QND scheme as

$$n_{\text{max}} = \frac{\bar{C}_2 - \bar{n}_{\text{th}}}{2\bar{n}_{\text{th}} + 1}. \quad (9)$$

Note that this equation implicitly requires that $\bar{C}_2 \geq \bar{n}_{\text{th}}$, which

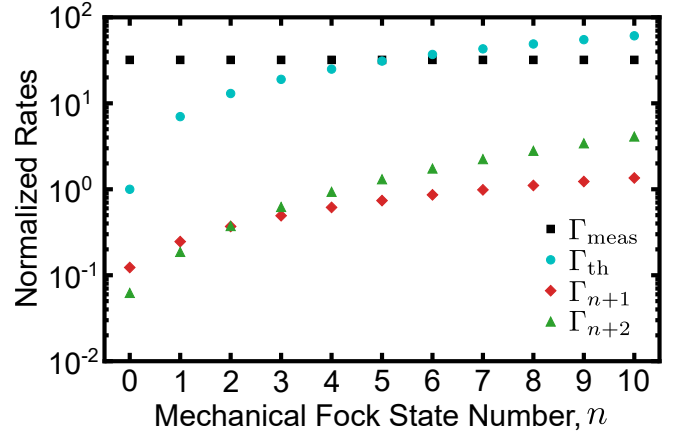


FIG. 2: Plot of the measurement rate, Γ_{meas} , and thermal decoherence rate, Γ_{th} , as well as the first- and second-order measurement-induced transition rates, Γ_{n+1} and Γ_{n+2} , normalized to the thermal decoherence rate of the ground state, $\Gamma_{\text{th}}^0 = \bar{n}_{\text{th}}\Gamma_{\text{m}}$, for the first ten Fock states of an optomechanical system. The system parameters are: $\omega_{\text{m}}/2\pi = 2$ GHz, $\Gamma_{\text{m}}/2\pi = 1$ kHz ($Q_{\text{m}} = 2 \times 10^6$), $\bar{n}_{\text{th}} = 0.25$ ($T \approx 60$ mK), $\kappa/2\pi = 500$ MHz, $\bar{N} = 100$, $g_1/2\pi = 50$ kHz, $g_2/2\pi = 100$ kHz. Here, $n_{\text{max}} \approx 5$ such that the first five mechanical Fock states can be monitored continuously using the QND measurement discussed in the main text.

as we shall see below, is ensured by Eq. (8).

The above analysis is valid for any arbitrary Fock state of the mechanical resonator. However, the minimum requirement necessary to perform a QND measurement of the mechanical oscillator's energy will occur when it is in the ground state, as Γ_{th} , $\Gamma_{n\pm 1}$ and $\Gamma_{n\pm 2}$ are all indeed minimized for $n = 0$ (see Fig. 2). In this situation, we are no longer concerned with rates corresponding to a reduction in phonon number (*i.e.* Γ_{n-1} , Γ_{n-2}), as the mechanical ground state is unable to emit phononic energy. Furthermore, in order to experimentally resolve shifts in the optical cavity resonance frequency due to the creation/annihilation of a single phonon, one often turns to a phase sensitive detection scheme, such as a Pound-Drever-Hall setup [23], where signal is maximized at $\Delta = 0$. Finally, we wish to operate in the sideband-resolved regime ($\omega_{\text{m}} \gg \kappa$), which as we shall see below is necessary for the QND measurements of the mechanical ground state. Under these circumstances, the rate hierarchy of Eq. (8) becomes

$$\Gamma_{\text{meas}} \gg \Gamma_{\text{th}}^0 \gg \Gamma_1, \Gamma_2, \quad (10)$$

where $\Gamma_{\text{th}}^0 = \bar{n}_{\text{th}}\Gamma_{\text{m}}$ is the rate at which the ground state of the mechanical resonator thermally decoheres, found by taking $n = 0$ in Eq. (S40). Furthermore, Γ_1 and Γ_2 are the measurement-induced rates associated with transitions to the first and second excited states from this ground state at $\Delta = 0$ and are given by

$$\begin{aligned} \Gamma_1 &= \frac{\bar{N}g_1^2\kappa}{\omega_{\text{m}}^2} = \frac{\bar{C}_1\Gamma_{\text{m}}\kappa^2}{4\omega_{\text{m}}^2}, \\ \Gamma_2 &= \frac{\bar{N}g_2^2\kappa}{8\omega_{\text{m}}^2} = \frac{\bar{C}_2\Gamma_{\text{m}}\kappa^2}{32\omega_{\text{m}}^2}, \end{aligned} \quad (11)$$

where similar to before we have introduced the first-order, cavity-enhanced cooperativity $\bar{C}_1 = \bar{N}C_1$ in terms of the corresponding first-order, single-photon cooperativity $C_1 = 4g_1^2/\kappa\Gamma_m$. Using these two expressions for Γ_1 and Γ_2 , the limits in Eq. (10) can also be recast in terms of the first- and second-order quantum cooperativities, $\mathcal{C}_1 = \bar{C}_1/\bar{n}_{\text{th}}$ and $\mathcal{C}_2 = \bar{C}_2/\bar{n}_{\text{th}}$ [20], as

$$\mathcal{C}_2 \gg 1 \gg \mathcal{C}_1 \left(\frac{\kappa^2}{4\omega_m^2} \right), \mathcal{C}_2 \left(\frac{\kappa^2}{32\omega_m^2} \right). \quad (12)$$

We now look to understand the fundamental limits associated with this type of QND measurement. First, by ensuring that $\Gamma_{\text{meas}} \gg \Gamma_2$ – that is to say we are able to measure the phonon state of the system before a measurement induces a transition to the second excited state – we arrive at the condition $32\omega_m^2 \gg \kappa^2$, which will certainly be satisfied for a sideband-resolved optomechanical system. Physically, this limit can be interpreted as the photons have a lifetime much larger than the mechanical period, such that they sample the mechanical motion over many oscillations before exiting the optical cavity. This is precisely the condition for the rotating wave approximation mentioned previously, whereby the rapidly oscillating, transition-inducing second-order terms in the Hamiltonian can be safely averaged to zero in favor of second-order terms that are constant in time.

Furthermore, the requirement that $\Gamma_{\text{meas}} \gg \Gamma_1$ allows us to set the following limit on the linear coupling with respect to the quadratic coupling

$$g_2 \gg g_1 \frac{\kappa}{2\omega_m}. \quad (13)$$

It is this limit that proves to be the most challenging to overcome when attempting to experimentally perform QND measurements of mechanical phonon number. By inspection of Eq. (13), we see that the sideband resolution condition discussed in the previous paragraph aids in suppressing the detrimental effect of linear coupling. A slightly more subtle observation is that since g_2 is proportional to x_{zpf}^2 while g_1 is linear in x_{zpf} , larger zero-point fluctuation amplitudes (corresponding to smaller effective masses and mechanical resonance frequencies) act to further relax the condition of requiring small linear coupling. We note that in order to satisfy this limit, the relative strengths of g_1 and g_2 (or equivalently G_1 and G_2) must be able to be tuned independently. This can be done for the system considered here by utilizing the relative symmetry between the optics and mechanics (see Supplementary Information). However, this is not the case for the quadratic coupling resulting from hybridization of two nearly degenerate optical modes found in MIM systems, where $g_2 = g_1^2/2\nu$, with ν being the coupling rate between the two optical modes (see Supplementary Information). In fact, one can put this relation into Eq. (13) to recover the single-photon strong-coupling requirement $g_1 \gg \kappa$, where we have assumed the limit $2\nu \gg \omega_m$ as is regularly done with MIM systems [2, 3, 5, 6]. Therefore, Eq. (13) provides a more general, less stringent condition for QND measurements of phonon number using a quadratically-coupled optomechanical cavity.

As a final note, we point out that even if the above conditions are satisfied, one must still satisfy the ground state linear- and quadratic-coupling conditions, *i.e.* $\Gamma_{\text{th}}^0 \gg \Gamma_1, \Gamma_2$. Therefore, the greater the sideband resolution and linear coupling suppression in a given system, the larger the difference between Γ_{meas} and both measurement-induced transition rates, Γ_1 and Γ_2 , producing a larger range of acceptable ground state thermal decoherence rates that will satisfy Eq. (10). Furthermore, we emphasize the importance of low occupation of the thermal bath. Even if one can cool the mechanical mode to near its ground state using active feedback cooling techniques [14, 18, 60, 61] in attempt to reduce Γ_{th} , it is not possible to reduce the thermal decoherence rate of the Fock state below $\Gamma_{\text{th}}^0 = \bar{n}_{\text{th}}\Gamma_m$. Therefore, passive cooling of an optomechanical system using a refrigeration system [62–65] will likely be necessary to facilitate these types of continuous QND measurements.

In this paper, we have investigated the limits involved with performing QND measurements of the quantized mechanical Fock states in an optomechanical cavity where quadratic coupling arises due to shared symmetries between a single optical and mechanical mode. By imposing the requirement that one measures the phononic state of the system faster than it thermally decoheres or transitions to another Fock state via the optomechanical interaction itself, it was shown that the single-photon strong-coupling condition associated with MIM systems can be circumvented. Instead a new, less stringent limit on the strength of the linear coupling was imposed, along with the rotating wave approximation in the form of optomechanical sideband resolution. With these conditions satisfied, such an optomechanical system could be used to perform quantum jump spectroscopy on the thermally-induced transitions between mechanical quanta [35]. One could also consider using this type of QND measurement to freeze the resonator into a given Fock state, prolonging its coherence time via the quantum Zeno effect [66], as has been demonstrated for trapped ions [67] and cold atoms [68, 69]. Such an effect could be useful for a number of optomechanical quantum information protocols [70, 71], where long coherence times are beneficial for applications such as quantum memories [17, 31] and transducers [72–75]. Furthermore, the ability to observe and manipulate the decoherence of these mesoscopic quantum mechanical states would provide a long sought-after experimental platform to aid in the understanding of the elusive quantum-to-classical transition.

Finally, we note that the type of QND measurements considered in this work could also be applied to electromechanical systems, as was considered recently in [76], where the authors arrive at results similar to that obtained in Eq. (13) of this paper.

Acknowledgments

The authors would like to thank Saeed Khan for bringing to our attention the master equation treatment that was used to calculate the rates in Eqs. (S40) and (5) (see Supplementary Information).

This work was supported by the University of Alberta, Faculty of Science; the Natural Sciences and Engineering Research Council, Canada (Grants Nos. RGPIN-2016-04523, DAS492947-2016, and STPGP 493807 - 16); and the Canada

Foundation for Innovation. B.D.H. acknowledges support from the Killam Trusts. A.M. acknowledges support from by the Deutsche Forschungsgemeinschaft through the Emmy Noether program (Grant No. ME 4863/1-1).

-
- [1] E. Joos, H. D. Zeh, C. Kiefer, D. J. W. Giulini, J. Kupsch, and I.-O. Stamatescu, *Decoherence and the Appearance of a Classical World in Quantum Theory* (Springer-Verlag, Berlin, 2003).
- [2] M. A. Schlosshauer, *Decoherence and the Quantum-to-Classical Transition* (Springer-Verlag, Berlin, 2007).
- [3] G. C. Ghirardi, A. Rimini, and T. Weber, *Phys. Rev. D* **34**, 470 (1986).
- [4] L. Diósi, *Phys. Rev. A* **40**, 1165 (1989).
- [5] R. Penrose, *Gen. Relativ. Gravit.* **28**, 581 (1996).
- [6] W. H. Zurek, *Rev. Mod. Phys.* **75**, 715 (2003).
- [7] S. Bose, K. Jacobs, and P. L. Knight, *Phys. Rev. A* **59**, 3204 (1999).
- [8] W. Marshall, C. Simon, R. Penrose, and D. Bouwmeester, *Phys. Rev. Lett.* **91**, 130401 (2003).
- [9] O. Romero-Isart, A. C. Pflanzer, F. Blaser, R. Kaltenbaek, N. Kiesel, M. Aspelmeyer, and J. I. Cirac, *Phys. Rev. Lett.* **107**, 020405 (2011).
- [10] Y. Chen, *J. Phys. B* **46**, 104001 (2013).
- [11] M. Aspelmeyer, T. J. Kippenberg, and F. Marquardt, *Rev. Mod. Phys.* **86**, 1391 (2014).
- [12] J. D. Thompson, B. M. Zwickl, A. M. Jayich, F. Marquardt, S. M. Girvin, and J. G. E. Harris, *Nature* **452**, 72 (2008).
- [13] A. A. Clerk, F. Marquardt, and J. G. E. Harris, *Phys. Rev. Lett.* **104**, 213603 (2010).
- [14] A. A. Gangat, T. M. Stace, and G. J. Milburn, *New J. Phys.* **13**, 043024 (2011).
- [15] M. R. Vanner, *Phys. Rev. X* **1**, 021011 (2011).
- [16] K. Børkje, *Phys. Rev. A* **90**, 023806 (2014).
- [17] R. Riedinger, S. Hong, R. A. Norte, J. A. Slater, J. Shang, A. G. Krause, V. Anant, M. Aspelmeyer, and S. Gröblacher, *Nature* **530**, 313 (2016).
- [18] J. D. Teufel, T. Donner, D. Li, J. W. Harlow, M. S. Allman, K. Cicak, A. J. Sirois, J. D. Whittaker, K. W. Lehnert, and R. W. Simmonds, *Nature* **475**, 359 (2011).
- [19] J. Chan, T. P. Mayer Alegre, A. H. Safavi-Naeini, J. T. Hill, A. Krause, S. Gröblacher, M. Aspelmeyer, and O. Painter, *Nature* **478**, 89 (2011).
- [20] A. H. Safavi-Naeini, J. Chan, J. T. Hill, T. P. Mayer Alegre, A. Krause, and O. Painter, *Phys. Rev. Lett.* **108**, 033602 (2012).
- [21] A. H. Safavi-Naeini, S. Gröblacher, J. T. Hill, J. Chan, M. Aspelmeyer, and O. Painter, *Nature* **500**, 185 (2013).
- [22] T. A. Palomaki, J. D. Teufel, R. W. Simmonds, and K. W. Lehnert, *Science* **342**, 710 (2013).
- [23] J. Suh, A. J. Weinstein, C. U. Lei, E. E. Wollman, S. K. Steinke, P. Meystre, A. A. Clerk, and K. C. Schwab, *Science* **344**, 1262 (2014).
- [24] A. J. Weinstein, C. U. Lei, E. E. Wollman, J. Suh, A. Metelmann, A. A. Clerk, and K. C. Schwab, *Phys. Rev. X* **4**, 041003 (2014).
- [25] E. E. Wollman, C. U. Lei, A. J. Weinstein, J. Suh, A. Kronwald, F. Marquardt, A. A. Clerk, and K. C. Schwab, *Science* **349**, 952 (2015).
- [26] J.-M. Pirkkalainen, E. Damskäg, M. Brandt, F. Massel, and M. A. Sillanpää, *Phys. Rev. Lett.* **115**, 243601 (2015).
- [27] F. Lecocq, J. B. Clark, R. W. Simmonds, J. Aumentado, and J. D. Teufel, *Phys. Rev. X* **5**, 041037 (2015).
- [28] C. U. Lei, A. J. Weinstein, J. Suh, E. E. Wollman, A. Kronwald, F. Marquardt, A. A. Clerk, and K. C. Schwab, *Phys. Rev. Lett.* **117**, 100801 (2016).
- [29] D. J. Wilson, V. Sudhir, N. Piro, R. Schilling, A. Ghadimi, and T. J. Kippenberg, *Nature* **524**, 325 (2015).
- [30] S. Hong, R. Riedinger, I. Marinković, A. Wallucks, S. G. Hofer, R. A. Norte, M. Aspelmeyer, and S. Gröblacher, *Science* **358**, 203 (2017).
- [31] A. P. Reed, K. H. Mayer, J. D. Teufel, L. D. Burkhardt, W. Pfaff, M. Reager, L. Sletten, X. Ma, R. J. Schoelkopf, E. Knill, and K. W. Lehnert, *Nat. Phys.* **13**, 1163 (2017).
- [32] R. Riedinger, A. Wallucks, I. Marinković, C. Löschnauer, M. Aspelmeyer, S. Hong, and S. Gröblacher, *Nature* **556**, 473 (2018).
- [33] C. F. Ockeleon-Korppi, E. Damskäg, J.-M. Pirkkalainen, M. Asjad, A. A. Clerk, F. Massel, M. J. Wooley, and M. A. Sillanpää, *Nature* **556**, 478 (2018).
- [34] J. C. Bergquist, R. G. Hulet, W. M. Itano, and D. J. Wineland, *Phys. Rev. Lett.* **57**, 1699 (1986).
- [35] S. Peil and G. Gabrielse, *Phys. Rev. Lett.* **83**, 1287 (1999).
- [36] G. Nogues, A. Rauschenbeutel, S. Osnaghi, M. Brune, J. M. Raimond, and S. Haroche, *Nature* **400**, 239 (1999).
- [37] S. Gleyzes, S. Kuhr, C. Guerlin, J. Bernu, S. Deléglise, U. B. Hoff, M. Brune, J.-M. Raimond, and S. Haroche, *Nature* **446**, 297 (2007).
- [38] P. Neumann, J. Beck, M. Steiner, F. Rempp, H. Fedder, P. R. Hemmer, J. Wrachtrup, and F. Jelezko, *Science* **329**, 542 (2010).
- [39] A. Lupaşcu, S. Saito, T. Picot, P. C. de Groot, C. J. P. M. Harmans, and J. E. Mooij, *Nat. Phys.* **3**, 119 (2007).
- [40] W. G. Unruh, *Phys. Rev. D* **18**, 1764 (1978).
- [41] V. B. Braginsky and F. Y. Khalili, *Quantum Measurement*, edited by K. S. Thorne (Cambridge University Press, Cambridge, 1995).
- [42] V. B. Braginsky, Y. I. Vorontsov, and K. S. Thorne, *Science* **209**, 547 (1980).
- [43] A. A. Clerk, M. H. Devoret, S. M. Girvin, F. Marquardt, and R. J. Schoelkopf, *Rev. Mod. Phys.* **82**, 1155 (2010).
- [44] A. M. Jayich, J. C. Sankey, B. M. Zwickl, C. Yang, J. D. Thompson, S. M. Girvin, A. A. Clerk, F. Marquardt, and J. G. E. Harris, *New J. Phys.* **10**, 095008 (2008).
- [45] J. C. Sankey, C. Yang, B. M. Zwickl, A. M. Jayich, and J. G. E. Harris, *Nat. Phys.* **6**, 707 (2010).
- [46] T. P. Purdy, D. W. C. Brooks, T. Botter, N. Brahms, Z.-Y. Ma, and D. M. Stamper-Kurn, *Phys. Rev. Lett.* **105**, 133602 (2010).
- [47] T. K. Paraíso, M. Kalae, L. Zang, H. Pfeifer, F. Marquardt, and O. Painter, *Phys. Rev. X* **5**, 041024 (2015).
- [48] M. Kalae, T. K. Paraíso, H. Pfeifer, and O. Painter, *Opt. Express* **24**, 21308 (2016).
- [49] H. Miao, S. Danilishin, T. Corbitt, and Y. Chen, *Phys. Rev. Lett.* **103**, 100402 (2009).
- [50] M. Ludwig, A. H. Safavi-Naeini, O. Painter, and F. Marquardt, *Phys. Rev. Lett.* **109**, 063601 (2012).
- [51] Y. Yanay, J. C. Sankey, and A. A. Clerk, *Phys. Rev. A* **93**,

- 063809 (2016).
- [52] H. Kaviani, C. Healey, M. Wu, R. Ghobadi, A. Hryciw, and P. E. Barclay, *Optica* **2**, 271 (2015).
 - [53] C. Doolin, B. D. Hauer, P. H. Kim, A. J. R. MacDonald, H. Ramp, and J. P. Davis, *Phys. Rev. A* **89**, 053838 (2014).
 - [54] B. D. Hauer, C. Doolin, K. S. D. Beach, and J. P. Davis, *Ann. Phys.* **339**, 181 (2013).
 - [55] D. H. Santamore, A. C. Doherty, and M. C. Cross, *Phys. Rev. B* **70**, 144301 (2004).
 - [56] C. W. Gardiner and P. Zoller, *Quantum Noise: A Handbook of Markovian and Non-Markovian Quantum Stochastic Methods with Applications to Quantum Optics* (Springer-Verlag, Berlin, 2004).
 - [57] F. Marquardt, J. P. Chen, A. A. Clerk, and S. M. Girvin, *Phys. Rev. Lett.* **99**, 093902 (2007).
 - [58] I. Martin and W. H. Zurek, *Phys. Rev. Lett.* **98**, 120401 (2007).
 - [59] E. D. Black, *Am. J. Phys.* **69**, 79 (2001).
 - [60] T. Rocheleau, T. Ndukum, C. Macklin, J. B. Hertzberg, A. A. Clerk, and K. C. Schwab, *Nature* **463**, 72 (2010).
 - [61] R. Rivière, S. Deléglise, S. Weis, E. Gavartin, O. Arcizet, A. Schliesser, and T. J. Kippenberg, *Phys. Rev. A* **83**, 063835 (2011).
 - [62] R. Rivière, O. Arcizet, A. Schliesser, and T. J. Kippenberg, *Rev. Sci. Instrum.* **84**, 043108 (2013).
 - [63] S. M. Meenehan, J. D. Cohen, S. Gröblacher, J. T. Hill, A. H. Safavi-Naeini, M. Aspelmeyer, and O. Painter, *Phys. Rev. A* **90**, 011803(R) (2014).
 - [64] A. J. R. MacDonald, G. G. Popowich, B. D. Hauer, P. H. Kim, A. Fredrick, X. Rojas, P. Doolin, and J.P. Davis, *Rev. Sci. Instrum.* **86**, 013107 (2015).
 - [65] A. J. R. MacDonald, B. D. Hauer, X. Rojas, P. H. Kim, G. G. Popowich, and J. P. Davis, *Phys. Rev. A* **93**, 013836 (2016).
 - [66] B Misra and E. C. G. Sudarshan, *J. Math. Phys.* **18**, 756 (1977).
 - [67] W. M. Itano, D. J. Heinzen, J. J. Bollinger, and D. J. Wineland, *Phys. Rev. A* **41**, 2295 (1990).
 - [68] M. C. Fischer, B. Gutiérrez-Medina, and M. G. Raizen, *Phys. Rev. Lett.* **87**, 040402 (2001).
 - [69] Y. S. Patil, S. Chakram, and M. Vengalattore, *Phys. Rev. Lett.* **115**, 140402 (2015).
 - [70] Y.-D. Wang and A. A. Clerk, *Phys. Rev. Lett.* **108**, 153603 (2012).
 - [71] K. Stannigel, P. Komar, S. J. M. Habraken, S. D. Bennett, M. D. Lukin, P. Zoller, and P. Rabl, *Phys. Rev. Lett.* **109**, 013603 (2012).
 - [72] J. T. Hill, A. H. Safavi-Naeini, J. Chan, and O. Painter, *Nat. Comm.* **3**, 1196 (2012).
 - [73] J. Bochmann, A. Vainsencher, D. D. Awschalom, and A. N. Cleland, *Nat. Phys.* **9**, 712 (2013).
 - [74] T. A. Palomaki, J. W. Harlow, J. D. Teufel, R. W. Simmonds, and K. W. Lehnert, *Nature* **495**, 210 (2013).
 - [75] R. W. Andrews, R. W. Peterson, T. P. Purdy, K. Cicak, R. W. Simmonds, C. A. Regal and K. W. Lehnert, *Nat. Phys.* **10**, 321 (2014).
 - [76] L. Dellantonio, O. Kyriienko, F. Marquardt, and A. S. Sørensen, *arXiv:1801.02438* (2018).

Supplementary Information for Phonon Quantum Nondemolition Measurements in Nonlinearly Coupled Optomechanical Cavities

I. OPTOMECHANICAL COUPLING TO TWO NEARLY DEGENERATE OPTICAL MODES

Here, we consider a mechanical resonator, with resonant angular frequency ω_m , position operator \hat{x} and phononic annihilation (creation) operators \hat{b} (\hat{b}^\dagger), that is simultaneously coupled to two optical modes, each of which are characterized by the annihilation (creation) operators \hat{a}_1 (\hat{a}_1^\dagger) and \hat{a}_2 (\hat{a}_2^\dagger), as well as the position-dependent angular frequencies $\omega_1(\hat{x})$ and $\omega_2(\hat{x})$. We also allow these two optical modes to be coupled to each other at a rate ν , which physically manifests itself as a photon tunneling rate between the optical modes to the left and right of the membrane in membrane-in-the-middle (MIM) systems [S1–S3] or a backscattering rate between clockwise and counterclockwise propagating modes in whispering gallery mode (WGM) optomechanics [S4]. The Hamiltonian for such an optomechanical system (ignoring the ground state energies, drive terms and interaction with the environment) will be given by

$$\hat{H} = \hbar\omega_1(\hat{x})\hat{a}_1^\dagger\hat{a}_1 + \hbar\omega_2(\hat{x})\hat{a}_2^\dagger\hat{a}_2 + \hbar\omega_m\hat{b}^\dagger\hat{b} + \hbar\nu(\hat{a}_1^\dagger\hat{a}_2 + \hat{a}_2^\dagger\hat{a}_1), \quad (\text{S1})$$

where the last term describes the interaction between the two optical modes, with a photon being annihilated in one while simultaneously created in the other. As was done in the main text, we expand each i th optical frequency to second order in mechanical position as

$$\omega_i(\hat{x}) = \omega_i + G_1^{(a_i)}\hat{x} + \frac{G_2^{(a_i)}}{2}\hat{x}^2, \quad (\text{S2})$$

where again we have the unperturbed optical frequency ω_i , as well as the first- and second-order optomechanical coupling coefficients, $G_1^{(a_i)}$ and $G_2^{(a_i)}$, with the superscript (a_i) allowing for one to identify the coupling coefficient associated with each optical mode. Inputting these expressions into Eq. (S1), we obtain the interaction Hamiltonian for the system

$$\begin{aligned} \hat{H} &= \hbar\omega_1\hat{a}_1^\dagger\hat{a}_1 + \hbar\omega_2\hat{a}_2^\dagger\hat{a}_2 + \hbar\omega_m\hat{b}^\dagger\hat{b} + \hbar\nu(\hat{a}_1^\dagger\hat{a}_2 + \hat{a}_2^\dagger\hat{a}_1) \\ &+ \hbar\left(G_1^{(a_1)}\hat{a}_1^\dagger\hat{a}_1 + G_1^{(a_2)}\hat{a}_2^\dagger\hat{a}_2\right)\hat{x} + \frac{\hbar}{2}\left(G_2^{(a_1)}\hat{a}_1^\dagger\hat{a}_1 + G_2^{(a_2)}\hat{a}_2^\dagger\hat{a}_2\right)\hat{x}^2. \end{aligned} \quad (\text{S3})$$

Choosing the optical modes to be degenerate (in the absence of coupling between them) such that $\omega_1 = \omega_2 = \omega_0$, we introduce the new basis with annihilation operators $\hat{a}_\pm = (\hat{a}_1 \pm \hat{a}_2)/\sqrt{2}$, which describes the two supermodes that emerge due to the avoided crossing between the two original degenerate optical modes. The new Hamiltonian in this supermode basis can then be written as

$$\begin{aligned} \hat{H} &= \hbar\omega_+\hat{a}_+^\dagger\hat{a}_+ + \hbar\omega_-\hat{a}_-^\dagger\hat{a}_- + \hbar\omega_m\hat{b}^\dagger\hat{b} + \hbar\left(\frac{G_1^{(a_1)} + G_1^{(a_2)}}{2}\right)(\hat{a}_+^\dagger\hat{a}_+ + \hat{a}_-^\dagger\hat{a}_-)\hat{x} \\ &+ \hbar\left(\frac{G_1^{(a_1)} - G_1^{(a_2)}}{2}\right)(\hat{a}_+^\dagger\hat{a}_- + \hat{a}_-^\dagger\hat{a}_+)\hat{x} + \hbar\left(\frac{G_2^{(a_1)} + G_2^{(a_2)}}{4}\right)(\hat{a}_+^\dagger\hat{a}_+ + \hat{a}_-^\dagger\hat{a}_-)\hat{x}^2 \\ &+ \hbar\left(\frac{G_2^{(a_1)} - G_2^{(a_2)}}{4}\right)(\hat{a}_+^\dagger\hat{a}_- + \hat{a}_-^\dagger\hat{a}_+)\hat{x}^2, \end{aligned} \quad (\text{S4})$$

where we now have the new supermode frequencies $\omega_\pm = \omega_0 \pm \nu$. The splitting between these two new supermodes is $\omega_+ - \omega_- = 2\nu$, such that each can be accessed individually if $\kappa_\pm < 2\nu$, with κ_\pm being the linewidth of the mode corresponding to a_\pm . Up to this point, we have not made any assumptions about the nature of the couplings in this system. In what follows, we will investigate how the Hamiltonian in Eq. (S4) can be used to effectively describe an optomechanical MIM system, as well as a mechanical element quadratically-coupled to an optical mode via shared symmetries.

In a conventional MIM optomechanical system, quadratic coupling arises due to the avoided crossing between the two hybridized optical supermodes mentioned above. Therefore, it is unnecessary to expand our optical frequencies to second order and we take $G_2^{(a_i)} = 0$ here. Furthermore, due to the geometry of MIM systems, as the mechanical elements is displaced, if the frequency of one optical mode increases, then the other mode's frequency will correspondingly decrease, leading to

$G_1^{(a_1)} = -G_1^{(a_2)} = G_1$ [S1, S3]. As we shall see, this difference in sign between the linear coupling of the two optical modes is crucial for generating quadratic coupling in these systems, as well as enforcing the single-photon strong-coupling condition associated with using them for quantum nondemolition (QND) measurements of mechanical Fock states [S2, S5, S6]. Applying these conditions to the general two-mode optomechanical Hamiltonian in Eq. (S4), we obtain the Hamiltonian for a MIM system as [S2, S3, S5–S7]

$$\hat{H}_{\text{MIM}} = \hbar\omega_+ \hat{a}_+^\dagger \hat{a}_+ + \hbar\omega_- \hat{a}_-^\dagger \hat{a}_- + \hbar\omega_m \hat{b}^\dagger \hat{b} + \hbar G_1 \left(\hat{a}_+^\dagger \hat{a}_- + \hat{a}_-^\dagger \hat{a}_+ \right) \hat{x}. \quad (\text{S5})$$

In this form, it is not obvious where the quadratic coupling arises in MIM systems. However, this system can be diagonalized, resulting in the Hamiltonian

$$\hat{H}_{\text{MIM}} = \hbar\omega'_+ \hat{d}_+^\dagger \hat{d}_+ + \hbar\omega'_- \hat{d}_-^\dagger \hat{d}_- + \hbar\omega_m \hat{b}^\dagger \hat{b}, \quad (\text{S6})$$

with corresponding eigenfrequencies

$$\omega'_\pm = \omega_0 \pm \sqrt{v^2 + G_1^2 \hat{x}^2}. \quad (\text{S7})$$

In the limit where $v \gg \omega_m$, \hat{x} can be treated as a quasistatic variable [S2, S3, S5, S6], allowing us to take $G_1 \hat{x} \ll v$. In this regime, the lowering operators of the diagonalized modes can be approximated as [S2]

$$\begin{aligned} \hat{d}_+ &\approx a_+ + \frac{G_1 \hat{x}}{2v} \hat{a}_-, \\ \hat{d}_- &\approx \frac{G_1 \hat{x}}{2v} a_+ - a_-, \end{aligned} \quad (\text{S8})$$

with the approximate frequencies

$$\omega'_\pm \approx \omega_0 \pm \left(v + \frac{G_1^2}{2v} \hat{x}^2 \right) = \omega_\pm \pm G_2' \hat{x}^2. \quad (\text{S9})$$

In this form, it is clear that these diagonalized mode frequencies exhibit a quadratic dependence on the position, with a coupling coefficient $G_2' = G_1^2/2v$. Furthermore, the operators d_\pm are formed by a linear combination of the supermode operators a_\pm , one of which is linearly coupled to the position variable \hat{x} . In this situation, even if we solely drive one of the supermodes, photons will tunnel to its counterpart and couple linearly to the mechanical resonator, causing its phononic Fock state to decohere. It is this process that leads to the requirement of the single-photon strong-coupling regime ($g_1 \gg \kappa$) required to perform QND measurements of phonon states in MIM optomechanical systems [S2, S5, S6].

We now consider an optomechanical system whereby the motion of the mechanical element shifts the frequencies of both optical modes in the same direction. Such a system could be realized as a nanomechanical resonator side-coupled to an optical WGM cavity [S8], with the two degenerate optical modes being the clockwise and counterclockwise propagating modes [S4]. In this case, the optomechanical coupling coefficients will be equal in both sign and magnitude, leading to $G_1^{(a_1)} = G_1^{(a_2)} = G_1$ and $G_2^{(a_1)} = G_2^{(a_2)} = G_2$. Note that we have opted to keep second-order terms in this analysis due to the fact that the avoided level crossing will no longer provide quadratic optomechanical coupling. Inserting these coefficients into the interaction Hamiltonian in Eq. (S4), we find

$$\hat{H}_{\text{WGM}} = \hbar\omega_+ \hat{a}_+^\dagger \hat{a}_+ + \hbar\omega_- \hat{a}_-^\dagger \hat{a}_- + \hbar\omega_m \hat{b}^\dagger \hat{b} + \hbar G_1 \left(\hat{a}_+^\dagger \hat{a}_+ + \hat{a}_-^\dagger \hat{a}_- \right) \hat{x} + \frac{\hbar G_2}{2} \left(\hat{a}_+^\dagger \hat{a}_+ + \hat{a}_-^\dagger \hat{a}_- \right) \hat{x}^2. \quad (\text{S10})$$

For this system, we are then left with a Hamiltonian that is already diagonalized. This has two very important consequences for this type of coupled system. First, the quadratic coupling that arose due to the avoided level crossing for the MIM system has vanished. However, there still exists quadratic coupling terms in our Hamiltonian as we have expanded the optical cavity resonance frequency to second order in mechanical position. Furthermore, as opposed to the MIM system, where the quadratic coupling is proportional to the square of the linear coupling, the second-order coupling coefficient here can be modified independently of the linear coupling by tuning the relative symmetry of the optical and mechanical modes shapes (see Sec. II). This leads us to the second important consequence of this system: since there is no linear mechanically-mediated coupling between the optical modes, QND measurements using this system are not constrained by the stringent single-photon strong-coupling regime. Instead, we obtain a limit on the linear coupling strength, G_1 , with respect to the quadratic coupling, G_2 , *i.e.* Eq. (13) in the main text.

We conclude this section by noting that in the main text, we assumed a single optical mode, as opposed to the coupled two-mode system considered here. The effect of adding a second, undriven optical mode to the system can be included in the optically-induced transition rates given by Eqs. (6) and (11) of the main text by taking $\bar{N} = \bar{N}_+ + \bar{N}_- = \bar{N}_1 + \bar{N}_2$, where $\bar{N}_i = \langle \hat{a}_i^\dagger \hat{a}_i \rangle$ is simply the average photon occupancy of the mode corresponding to \hat{a}_i . For such a system, if one drives the \hat{a}_1 mode (call it the clockwise mode) to a photon occupancy \hat{N}_1 , then backscattering will cause the \hat{a}_2 mode (counterclockwise mode) to be populated to an occupancy [S9]

$$\bar{N}_2 = \frac{v^2}{\Delta^2 + (\kappa/2)^2} \bar{N}_1. \quad (\text{S11})$$

For the $\Delta = 0$ condition associated with the phase sensitive measurements discussed in the main text, we then have $\bar{N}_2 = (2v/\kappa)^2 \bar{N}_1$. For $2v \ll \kappa$, $\bar{N}_2 \ll \bar{N}_1$, that is the counterclockwise mode is essentially unpopulated such that we can take $\bar{N} \approx \bar{N}_1$. Therefore, in this regime, we need only consider one mode (in this case the clockwise mode). We note that in this situation a small, but finite leakage of photons into the counterclockwise mode will not lead to accelerated decoherence associated with the MIM system [S5] due to the fact that counterclockwise photons interact with the mechanics in the same way clockwise photons do.

For the case where $2v \gg \kappa$, the situation is complicated by the fact that the clockwise and counterclockwise modes hybridize into the two individually accessible symmetric and antisymmetric modes corresponding to \hat{a}_\pm . Under these circumstances, the resonant probing condition required for phase sensitive measurements results in $\Delta = \pm v$. In either case this leads to $\bar{N}_2 \approx \bar{N}_1$, meaning that even though we are only driving the clockwise mode, strong backscattering ensures that in equilibrium both modes are equally populated. Again, due to the fact that photons in the clockwise and counterclockwise modes interact identically with the mechanics, this photon redistribution does nothing to affect the optically-induced transition rates. However, as half of the photons now reside in the unmonitored counterclockwise mode, the measurement rate is halved. Therefore, a single mode treatment is still valid in this regime, provided we account for this factor of two decrease in the measurement rate of the mechanical phonon number.

II. OPTOMECHANICAL COUPLING USING NON-DEGENERATE PERTURBATION THEORY

Here we use the perturbative approach developed by Johnson *et al.* [S10] to determine the first- and second-order optomechanical coupling coefficients for mechanical systems coupled to non-degenerate optical modes. In doing so, we will show that it is possible, in principle, to completely eliminate linear coupling in favor of quadratic coupling by exploiting the symmetry of an optomechanical system.

We begin by considering a high- Q optical mode with a resonance angular frequency ω_i , such that we can approximate the time-dependence of the mode's electric field as $\vec{E}_i(\vec{r}, t) = e^{i\omega_i t} \vec{E}_i(\vec{r})$. Using Maxwell's equations for a source-free dielectric, as is relevant for the optomechanical systems considered here, one obtains the Helmholtz equation for the electric field as

$$\nabla^2 |E_i\rangle = -\frac{\omega_i^2 \epsilon_r(\vec{r})}{c^2} |E_i\rangle, \quad (\text{S12})$$

where ∇^2 is the Laplacian operator and the geometry of the resonator is specified by its spatially-varying relative permittivity profile $\epsilon_r(\vec{r})$. We have also chosen to follow the notation of Johnson *et al.* by representing the electric field of the cavity mode using the Dirac bracket state vectors $|E_i\rangle = \vec{E}_i(\vec{r})$, which have an inner product defined as

$$\langle E_i | E_j \rangle \equiv \int \vec{E}_i^*(\vec{r}) \cdot \vec{E}_j(\vec{r}) dV, \quad (\text{S13})$$

where the integral is performed over the volume of the optomechanical system [S10]. With this definition, the optical modes of the cavity are orthogonal in the sense that $\langle E_i | \epsilon_r | E_j \rangle = \langle E_i | \epsilon_r | E_i \rangle \delta_{ij}$.

We now imagine introducing a small shift in the cavity's permittivity profile, resulting in $\epsilon(\vec{r}) \rightarrow \epsilon(\vec{r}) + \delta\epsilon(\vec{r})$. Treating the problem perturbatively, we determine the new electric fields $|E'_i\rangle$, and their corresponding frequencies ω'_i , in this shifted geometry by expanding to second order as

$$|E'_i\rangle = |E_i^{(0)}\rangle + |E_i^{(1)}\rangle + |E_i^{(2)}\rangle, \quad (\text{S14a})$$

$$\omega'_i = \omega_i^{(0)} + \omega_i^{(1)} + \omega_i^{(2)}. \quad (\text{S14b})$$

Here the superscript (0) indicates the original unperturbed quantity, while the (1) and (2) indicate the first- and second-order corrections, proportional to $\delta\epsilon$ and $(\delta\epsilon)^2$, respectively. We note that these higher order corrections to the electric field are chosen

to be orthogonal to the unperturbed field in the same sense as before such that $\langle E_i^{(0)} | \epsilon_r | E_i^{(n>0)} \rangle = 0$.

For perturbations that are optomechanical in nature, the shift of the dielectric profile will be induced due to the motion of a mechanical element. In this case, we can also expand the optical mode frequency to second order in a similar fashion to Eq. (S2) as

$$\omega'_i = \omega_i + G_1 \Delta x + \frac{G_2}{2} (\Delta x)^2, \quad (\text{S15})$$

where Δx is the resonator's displacement from equilibrium. Matching these terms with the ones found in Eq. (S14b), Eq. (S12) can be solved order-by-order to find [S10–S13]

$$\omega_i = \omega_i^{(0)}, \quad (\text{S16a})$$

$$G_1 = \frac{\omega^{(1)}}{\Delta x} = -\frac{\omega^{(0)}}{2} \frac{\langle E_i^{(0)} | \frac{d\epsilon_r}{dx} | E_i^{(0)} \rangle}{\langle E_i^{(0)} | \epsilon_r | E_i^{(0)} \rangle}, \quad (\text{S16b})$$

$$G_2 = \frac{\omega^{(2)}}{(\Delta x)^2} = \frac{3G_1^2}{\omega_i} + \sum_{\omega_j \neq \omega_i} G_{ij}, \quad (\text{S16c})$$

where the sum is performed over all other optical cavity modes and

$$G_{ij} = \frac{\omega_i^3}{\omega_i^2 - \omega_j^2} \frac{|\langle E_j^{(0)} | \frac{d\epsilon_r}{dx} | E_i^{(0)} \rangle|^2}{\langle E_i^{(0)} | \epsilon_r | E_i^{(0)} \rangle \langle E_j^{(0)} | \epsilon_r | E_j^{(0)} \rangle}. \quad (\text{S17})$$

Upon inspection of Eq. (S16b), we see that linear coupling is proportional to the self-overlap of the optical mode, mediated by the change in relative permittivity with respect to the mechanical displacement, x . Meanwhile, in Eq. (S16c) we see that the quadratic coupling exhibits both a self-overlap term, as well as a term depending on the cross-coupling between the original unperturbed modes and the spectrum of other non-degenerate cavity modes (the case of quadratic coupling in degenerate cavity modes was discussed in Sec. I). Therefore, linear optomechanical coupling will in principle be zero if the field self-overlap term vanishes, that is $\langle E_i^{(0)} | \frac{d\epsilon_r}{dx} | E_i^{(0)} \rangle = 0$ [S13]. Furthermore, in this situation the quadratic coupling is given by

$$G_2 = \sum_{\omega_j \neq \omega_i} G_{ij}, \quad (\text{S18})$$

with only the cross-coupling terms surviving. Therefore, provided these terms do not sum to zero, a non-zero quadratic coupling can be achieved in the absence of linear coupling [S13].

To better understand the physical conditions that lead to vanishing linear optomechanical coupling, we investigate the case where the optomechanical coupling is due to shifting the boundary conditions of the optical mode (as opposed to the photoelastic effect [S14]), pertinent to the majority of optomechanical systems. For this situation, we find that [S10, S11]

$$\langle E_i | \frac{d\epsilon_r}{dx} | E_j \rangle = \int (\vec{q}(\vec{r}) \cdot \vec{u}) \left[\Delta\epsilon \vec{E}_i^{\parallel*} \cdot \vec{E}_j^{\parallel} - \Delta\epsilon^{-1} \vec{D}_i^{\perp*} \cdot \vec{D}_j^{\perp} \right] dA, \quad (\text{S19})$$

where $\vec{q}(\vec{r})$ is the mechanical modeshape function and $\vec{D} = \epsilon_0 \epsilon_r \vec{E}$ is the electric displacement field. The integral is performed over the surface of the unperturbed optical resonator as defined by its unit normal vector \vec{u} . We also have introduced the superscripts \parallel and \perp to denote the components of the associated fields parallel and perpendicular to the cavity surface. Finally, $\Delta\epsilon = \epsilon_d - \epsilon_s$ and $\Delta\epsilon^{-1} = \epsilon_d^{-1} - \epsilon_s^{-1}$, where ϵ_d and ϵ_s are the relative permittivities of the optomechanical device's material and the surrounding medium, respectively.

The expression in Eq. (S19) will be zero if the integrand is an odd function with respect to the symmetry axes of the optical cavity. In practice, this can be realized by implementing an optical intensity profile that exhibits even symmetry, along with a mechanical modeshape (after dot product with the unit surface normal) that demonstrates odd symmetry [S13]. This amounts to having an optical field which is unable to distinguish the direction of motion of the mechanics, that is the optical frequency shift is even with respect to mechanical displacement. Therefore, the first term in the cavity expansion (ignoring the zeroth-order term corresponding to the unperturbed cavity frequency) must be proportional to $(\Delta x)^2$, leading to quadratic optomechanical coupling.

III. DECOHERENCE RATES ASSOCIATED WITH OPTOMECHANICAL QND MEASUREMENTS OF MECHANICAL FOCK STATES

Here we use a master equation approach to determine the relevant measurement-induced and thermal decoherence rates associated with the optomechanical QND measurement considered in the main text. We begin by considering an optical cavity mode that is coupled to a mechanical mode with resonant frequency ω_m and a Markovian bath; the latter of which gives rise to a cavity decay rate κ . This system will be described by the Hamiltonian

$$\hat{H} = \hat{H}_c + \hat{H}_m + \hat{H}_{om} + \hat{H}_\kappa + \hat{H}_\Gamma, \quad (\text{S20a})$$

$$\hat{H}_c = \hbar\Delta\hat{d}^\dagger\hat{d}, \quad (\text{S20b})$$

$$\hat{H}_m = \hbar\omega_m\hat{b}^\dagger\hat{b}, \quad (\text{S20c})$$

$$\hat{H}_{om} = \hbar\bar{a} \left[g_1 (\hat{b} + \hat{b}^\dagger) + \frac{g_2}{2} (\hat{b}\hat{b} + \hat{b}^\dagger\hat{b}^\dagger) \right] (\hat{d} + \hat{d}^\dagger), \quad (\text{S20d})$$

where g_1 and g_2 are the single photon, single phonon and single photon, two phonon optomechanical coupling rates defined in the main text. Here, we have also assumed that the cavity is driven via an external drive with frequency ω_d , displacing the optical cavity operators according to $\hat{a} = \bar{a} + \hat{d}$, where the \bar{a} is the classical amplitude (taken to be real) and \hat{d} denotes the cavity fluctuations. We neglect terms proportional to $\hat{d}^\dagger\hat{d}$ in the interaction Hamiltonian \hat{H}_{om} . In addition, we assume that we are in a rotated frame for the cavity mode with respect to an external drive and we account for a static shift induced by the mechanics, *i.e.* the optical detuning is given by $\Delta = \omega_c - \omega_d + g_2(\bar{n} + \frac{1}{2})$, where $\bar{n} = \langle \hat{n} \rangle$. Finally, the dissipative baths for the optical cavity and mechanical resonator are described as usual and denoted by \hat{H}_κ and \hat{H}_Γ , respectively.

The dynamics of the system is then captured by the master equation, written in superoperator notation as [S15]

$$\frac{\partial}{\partial t}\hat{\rho} = (\mathcal{L}_c + \mathcal{L}_m + \mathcal{L}_{om})\hat{\rho}, \quad (\text{S21})$$

with $\hat{\rho}$ being the total density matrix of the system (including both optical and mechanical components). Here, we have defined the superoperators

$$\mathcal{L}_c = -\frac{i}{\hbar}[\hat{H}_c, \bullet] + \frac{\kappa}{2}\mathcal{D}[\hat{d}]\bullet, \quad (\text{S22a})$$

$$\mathcal{L}_m = -\frac{i}{\hbar}[\hat{H}_m, \bullet] + \frac{\Gamma_m}{2} \{ (\bar{n}_{th} + 1) \mathcal{D}[\hat{b}] + \bar{n}_{th} \mathcal{D}[\hat{b}^\dagger] \} \bullet, \quad (\text{S22b})$$

$$\mathcal{L}_{om} = -\frac{i}{\hbar}[\hat{H}_{om}, \bullet], \quad (\text{S22c})$$

$$\mathcal{D}[\hat{o}]\bullet = 2\hat{o}\bullet\hat{o}^\dagger - \hat{o}^\dagger\hat{o}\bullet - \bullet\hat{o}^\dagger\hat{o} = [\hat{o}, \bullet\hat{o}^\dagger] + [\hat{o}\bullet, \hat{o}^\dagger], \quad (\text{S22d})$$

where \bullet is a placeholder for the operator the superoperator is acting upon and \hat{o} is a generic ladder operator. We note that we have also assumed a zero-temperature bath for the cavity.

We can now move into a new interaction picture

$$\hat{\rho}' = e^{-(\mathcal{L}_c + \mathcal{L}_m)t}\hat{\rho} \quad \Rightarrow \quad \frac{\partial\hat{\rho}'}{\partial t} = e^{-(\mathcal{L}_c + \mathcal{L}_m)t}\mathcal{L}_{om}e^{(\mathcal{L}_c + \mathcal{L}_m)t}\hat{\rho}' \equiv \mathcal{L}'_{om}(t)\hat{\rho}', \quad (\text{S23})$$

where we have simply used the product rule and Eq. (S21) to derive the master equation for $\hat{\rho}'$. This master equation can be formally integrated to obtain the solution

$$\hat{\rho}'(t) = \hat{\rho}'(0) + \int_0^t d\tau \mathcal{L}'_{om}(\tau)\hat{\rho}'(\tau), \quad (\text{S24})$$

which can be substituted back into Eq. (S23) and, by additionally performing the trace over the cavity space, we arrive at the new master equation

$$\frac{\partial}{\partial t}\text{Tr}_c\{\hat{\rho}'(t)\} \equiv \frac{\partial\hat{\rho}'_m}{\partial t} = \text{Tr}_c\{\mathcal{L}'_{om}(t)\hat{\rho}'(0)\} + \int_0^t d\tau \text{Tr}_c\{\mathcal{L}'_{om}(t)\mathcal{L}'_{om}(\tau)\hat{\rho}'(\tau)\}. \quad (\text{S25})$$

Thus we have to calculate

$$\mathcal{L}'_{om} = -i\bar{a} [\mathcal{A}(t)\mathcal{B}(t) - \mathcal{A}^\dagger(t)\mathcal{B}^\dagger(t)], \quad (\text{S26})$$

where

$$\mathcal{A}(t) = e^{-\mathcal{L}t} (\hat{d} + \hat{d}^\dagger) \bullet e^{\mathcal{L}t}, \quad (\text{S27a})$$

$$\mathcal{B}(t) = e^{-\mathcal{L}_m t} \hat{B} \bullet e^{\mathcal{L}_m t}, \quad (\text{S27b})$$

and we have introduced the operator $\hat{B} = g_1 (\hat{b} + \hat{b}^\dagger) + \frac{g_2}{2} (\hat{b}\hat{b} + \hat{b}^\dagger\hat{b}^\dagger)$. Note that \hat{B} and $(\hat{d} + \hat{d}^\dagger)$ are Hermitian, but we have $(\hat{d}\bullet)^\dagger = \bullet\hat{d}^\dagger$, hence the appearance of $\mathcal{A}^\dagger(t)$ and $\mathcal{B}^\dagger(t)$. To further evaluate the superoperator \mathcal{L}'_{om} , we need the dynamics of the cavity operator in this interaction picture:

$$\mathcal{A}(t) = \hat{d} \bullet e^{-(i\Delta + \frac{\kappa}{2})t} + \hat{d}^\dagger \bullet e^{(i\Delta + \frac{\kappa}{2})t} - \bullet\hat{d}^\dagger e^{i\Delta t} \left(e^{\frac{\kappa}{2}t} - e^{-\frac{\kappa}{2}t} \right). \quad (\text{S28})$$

So far we have not made any approximations, the above treatment resembles the standard derivation for a master equation. We now assume that the optical cavity and mechanical resonator are uncorrelated at all times, so that the density matrix factorizes as $\hat{\rho} \equiv \hat{\rho}_m \otimes \hat{\rho}_c$ [S16], where $\hat{\rho}_c$ denotes the density matrix of the cavity-mode. We also make a Born approximation and assume that the cavity mode fluctuations \hat{d} are not affected by the dynamics of the mechanics, that is we set $\hat{\rho}_c(t) \approx \hat{\rho}_c(0)$. This means that the total density matrix remains a product of the initial cavity density matrix and the mechanical density matrix, *i.e.* $\hat{\rho}'(t) \approx \hat{\rho}'_m(t) \otimes \hat{\rho}_c(0) \equiv \hat{\rho}'_m(t) \otimes |0\rangle\langle 0|$ (for the cavity being in the vacuum state in this displaced frame). Under this assumption the first term in Eq. (S25) vanishes and with

$$\text{Tr}_c \{ \mathcal{A}(t) \mathcal{A}(\tau) |0\rangle\langle 0| \} = \text{Tr}_c \{ \mathcal{A}^\dagger(t) \mathcal{A}(\tau) |0\rangle\langle 0| \} = e^{-(i\Delta + \frac{\kappa}{2})(t-\tau)}, \quad (\text{S29a})$$

$$\text{Tr}_c \{ \mathcal{A}^\dagger(t) \mathcal{A}^\dagger(\tau) |0\rangle\langle 0| \} = \text{Tr}_c \{ \mathcal{A}(t) \mathcal{A}(\tau) |0\rangle\langle 0| \} = e^{+(i\Delta - \frac{\kappa}{2})(t-\tau)}, \quad (\text{S29b})$$

we can evaluate the second term as

$$\text{Tr}_c \{ \mathcal{L}'_{\text{om}}(t) \mathcal{L}'_{\text{om}}(\tau) \hat{\rho}'(\tau) \} = -\bar{N} \left[\{ \mathcal{B}(t) \mathcal{B}(\tau) - \mathcal{B}^\dagger(t) \mathcal{B}(\tau) \} e^{-(i\Delta + \frac{\kappa}{2})(t-\tau)} + \text{h.c.} \right] \hat{\rho}'_m(\tau). \quad (\text{S30})$$

Here

$$\bar{N} = \frac{\kappa_e}{\Delta^2 + (\kappa/2)^2} \frac{P}{\hbar\omega_d}, \quad (\text{S31})$$

is the average intracavity photon number, with κ_e and P being the optical cavity's external decay rate and input power. Using the expression in Eq. (S30), the master equation yields (with change of variables $t' = t - \tau$)

$$\frac{\partial \hat{\rho}'_m}{\partial t} = -\bar{N} \int_0^t dt' \left[\{ \mathcal{B}(t) \mathcal{B}(t-t') - \mathcal{B}^\dagger(t) \mathcal{B}(t-t') \} e^{-(i\Delta + \frac{\kappa}{2})t'} + \text{h.c.} \right] \hat{\rho}'_m(t-t'), \quad (\text{S32})$$

which we can transform back knowing that $\hat{\rho}_m(t) = e^{\mathcal{L}_m t} \hat{\rho}'_m(t)$ and move into an interaction picture with respect to the free mechanical Hamiltonian. This all gives us

$$\begin{aligned} \frac{\partial \hat{\rho}_m}{\partial t} &= -\bar{N} \int_0^t dt' \left(\left\{ g_1^2 \left[\{ \hat{b}\hat{b}^\dagger \bullet - \hat{b}^\dagger \bullet \hat{b} \} e^{-i\omega_m t'} + \{ \hat{b}^\dagger \hat{b} \bullet - \hat{b} \bullet \hat{b}^\dagger \} e^{+i\omega_m t'} \right] e^{-(i\Delta + \frac{\kappa}{2})t'} \right. \right. \\ &+ \frac{g_2^2}{4} \left[\{ \hat{b}\hat{b}\hat{b}^\dagger \hat{b}^\dagger \bullet - \hat{b}^\dagger \hat{b}^\dagger \bullet \hat{b}\hat{b} \} e^{-i2\omega_m t'} + \{ \hat{b}^\dagger \hat{b}^\dagger \hat{b}\hat{b} \bullet - \hat{b}\hat{b} \bullet \hat{b}^\dagger \hat{b}^\dagger \} e^{+i2\omega_m t'} \right] e^{-(i\Delta + \frac{\kappa}{2})t'} \left. \right\} + \text{h.c.} \Big) \hat{\rho}_m(t-t') \\ &+ \frac{\Gamma_m}{2} \{ (\bar{n}_{\text{th}} + 1) \mathcal{D}[\hat{b}] + \bar{n}_{\text{th}} \mathcal{D}[\hat{b}^\dagger] \} \hat{\rho}_m(t), \end{aligned} \quad (\text{S33})$$

where we have also applied the rotating wave approximation. In the next step we apply a Markov approximation and solve the integrals for $t \rightarrow \infty$, obtaining

$$\begin{aligned} \frac{\partial \hat{\rho}_m}{\partial t} &= -\frac{i\bar{N}}{\hbar} [\hat{H}_r, \hat{\rho}_m(t)] + \bar{N} \left(g_1^2 \Re \{ \chi_c(\omega_m) \} \mathcal{D}[\hat{b}^\dagger] + g_1^2 \Re \{ \chi_c(-\omega_m) \} \mathcal{D}[\hat{b}] \right. \\ &+ \frac{g_2^2}{4} \Re \{ \chi_c(2\omega_m) \} \mathcal{D}[\hat{b}^\dagger \hat{b}^\dagger] + \frac{g_2^2}{4} \Re \{ \chi_c(-2\omega_m) \} \mathcal{D}[\hat{b}\hat{b}] \Big) \hat{\rho}_m(t) \\ &+ \frac{\Gamma_m}{2} \{ (\bar{n}_{\text{th}} + 1) \mathcal{D}[\hat{b}] + \bar{n}_{\text{th}} \mathcal{D}[\hat{b}^\dagger] \} \hat{\rho}_m(t). \end{aligned} \quad (\text{S34})$$

Here, $\chi_c(\omega) = [i(\Delta + \omega) + \kappa/2]^{-1}$ is the susceptibility of the optical cavity and the coherent dynamics are described by the Hamiltonian

$$\hat{H}_r = \hbar g_1^2 (\Im \{\chi_c(\omega_m)\} + \Im \{\chi_c(-\omega_m)\}) \hat{b}^\dagger \hat{b} + \frac{\hbar g_2^2}{4} (\Im \{\chi_c(2\omega_m)\} \hat{b} \hat{b} \hat{b}^\dagger \hat{b}^\dagger + \Im \{\chi_c(-2\omega_m)\} \hat{b}^\dagger \hat{b}^\dagger \hat{b} \hat{b}), \quad (\text{S35})$$

where the first term describes a shift induced by the linear coupling, while the second term is of the Kerr-type (Lamb shift). The real and imaginary part of the optical susceptibility can be expressed as

$$\Re \{\chi_c(\omega)\} = \frac{\kappa/2}{(\omega + \Delta)^2 + (\kappa/2)^2}, \quad (\text{S36a})$$

$$\Im \{\chi_c(\omega)\} = -\frac{(\omega + \Delta)}{(\omega + \Delta)^2 + (\kappa/2)^2}, \quad (\text{S36b})$$

where we note that $\Re \{\chi_c(\omega)\} = S_{NN}(-\omega)/2\bar{N}$, with

$$S_{NN}(\omega) = \frac{\bar{N}\kappa}{(\omega - \Delta)^2 + (\kappa/2)^2}, \quad (\text{S37})$$

being the photon number spectral density [S17–S20].

We now use the fact that we can determine the probability, p_n , of being in the n th Fock state by taking the inner product of the density matrix using the number state basis vectors, that is $p_n(t) = \langle n | \hat{\rho}_m(t) | n \rangle$. If we assume that we are initially in the n th Fock state, such that $p_n(0) = 1$, then the total rate at which we decohere from that pure state can be found using Eq. (S34) as

$$|\dot{p}_n| = |\langle n | \dot{\rho}_m | n \rangle| = \Gamma_{n+1} + \Gamma_{n-1} + \Gamma_{n+2} + \Gamma_{n-2} + \Gamma_{\text{th}}, \quad (\text{S38})$$

where

$$\begin{aligned} \Gamma_{n+1} &= (n+1)g_1^2 S_{NN}(-\omega_m), \\ \Gamma_{n-1} &= ng_1^2 S_{NN}(\omega_m), \\ \Gamma_{n+2} &= (n+1)(n+2) \frac{g_2^2}{4} S_{NN}(-2\omega_m), \\ \Gamma_{n-2} &= n(n-1) \frac{g_2^2}{4} S_{NN}(2\omega_m), \end{aligned} \quad (\text{S39})$$

are the rates due to by measurement-induced transitions from $n \rightarrow n \pm 1$ and $n \rightarrow n \pm 2$, while

$$\Gamma_{\text{th}} = \Gamma_m [(\bar{n}_{\text{th}} + 1)n + \bar{n}_{\text{th}}(n+1)], \quad (\text{S40})$$

is the rate associated the thermal decoherence rate of the n th Fock state of the mechanical resonator due to coupling with the external bath [S21, S22].

IV. SIGNAL-TO-NOISE RATIO OF QND PHONON MEASUREMENT USING A POUND-DREVER-HALL DETECTION SYSTEM

Here, we consider the signal-to-noise ratio for a phase-sensitive measurement using a Pound-Drever-Hall detection system in the context of performing an optomechanical QND measurement of mechanical energy quantization. For Pound-Drever-Hall detection, the shot noise limited angular frequency spectral density of this system will be given by $S_\omega = \kappa/4\bar{N}$ [S18, S23]. As expected, the shot noise is decreased as we add photons to the system, as well as when we reduce the linewidth of our resonance, narrowing the uncertainty in the cavity frequency. In order to resolve the frequency shift due a single phonon in our mechanical resonator, we require its spectral density to exceed this noise level. Assuming that the lifetime of our phonon state is thermally-limited, this spectral density will simply be given by $S_{\text{phon}} = 4g_2^2/\Gamma_{\text{th}}$ [S18]. The signal-to-noise ratio for such a measurement is then given by

$$\eta = \frac{S_{\text{phon}}}{S_\omega} = \frac{16\bar{N}g_2^2}{\kappa\Gamma_{\text{th}}}. \quad (\text{S41})$$

In order to measure a shift in the optical cavity frequency due to the change of a single phonon in the occupancy of our mechanical resonator, we require this ratio to be greater than one. Fortunately, this condition is guaranteed by the requirement that $\Gamma_{\text{meas}} \gg \Gamma_{\text{th}}$ given in Eq. (8) of the main text, which ensures that $4\sqrt{N}g_2^2/\kappa\Gamma_{\text{th}} \gg 1$, and therefore $\eta > 1$.

-
- [S1] A. M. Jayich, J. C. Sankey, B. M. Zwickl, C. Yang, J. D. Thompson, S. M. Girvin, A. A. Clerk, F. Marquardt, and J. G. E. Harris, *New J. Phys.* **10**, 095008 (2008).
- [S2] M. Ludwig, A. H. Safavi-Naeini, O. Painter, and F. Marquardt, *Phys. Rev. Lett.* **109**, 063601 (2012).
- [S3] T. K. Paraíso, M. Kalae, L. Zang, H. Pfeifer, F. Marquardt, and O. Painter, *Phys. Rev. X* **5**, 041024 (2015).
- [S4] T. J. Kippenberg, S. M. Spillane, and K. J. Vahala, *Opt. Lett.* **27**, 1669 (2002).
- [S5] H. Miao, S. Danilishin, T. Corbitt, and Y. Chen, *Phys. Rev. Lett.* **103**, 100402 (2009).
- [S6] Y. Yanay, J. C. Sankey, and A. A. Clerk, *Phys. Rev. A* **93**, 063809 (2016).
- [S7] M. Kalae, T. K. Paraíso, H. Pfeifer, and O. Painter, *Opt. Express* **24**, 21308 (2016).
- [S8] C. Doolin, B. D. Hauer, P. H. Kim, A. J. R. MacDonald, H. Ramp, and J. P. Davis, *Phys. Rev. A* **89**, 053838 (2014).
- [S9] D. J. Wilson, V. Sudhir, N. Piro, R. Schilling, A. Ghadimi, and T. J. Kippenberg, *Nature* **524**, 325 (2015).
- [S10] S. G. Johnson, M. Ibanescu, M. A. Skorobogatiy, O. Weisberg, J. D. Joannopoulos, and Y. Fink, *Phys. Rev. E* **65**, 066611 (2002).
- [S11] M. Eichenfield, J. Chan, A. H. Safavi-Naeini, K. J. Vahala, and O. Painter, *Opt. Express* **17**, 20078 (2009).
- [S12] A. W. Rodriguez, A. P. McCauley, P.-C. Hui, D. Woolf, E. Iwase, F. Capasso, M. Loncar, and S. G. Johnson, *Opt. Express* **19**, 2225 (2011).
- [S13] H. Kaviani, C. Healey, M. Wu, R. Ghobadi, A. Hryciw, and P. E. Barclay, *Optica* **2**, 271 (2014).
- [S14] J. Chan, T. P. Mayer Alegre, A. H. Safavi-Naeini, J. T. Hill, A. Krause, S. Gröblacher, M. Aspelmeyer, and O. Painter, *Nature* **478**, 89 (2011).
- [S15] H. J. Carmichael, *Statistical Methods in Quantum Optics 2: Non-Classical Fields* (Springer-Verlag, Berlin, 2008).
- [S16] I. Martin and W. H. Zurek, *Phys. Rev. Lett.* **98**, 120401 (2007).
- [S17] F. Marquardt, J. P. Chen, A. A. Clerk, and S. M. Girvin, *Phys. Rev. Lett.* **99**, 093902 (2007).
- [S18] J. D. Thompson, B. M. Zwickl, A. M. Jayich, F. Marquardt, S. M. Girvin, and J. G. E. Harris, *Nature* **452**, 72 (2008).
- [S19] A. A. Clerk, M. H. Devoret, S. M. Girvin, F. Marquardt, and R. J. Schoelkopf, *Rev. Mod. Phys.* **82**, 1155 (2010).
- [S20] M. Aspelmeyer, T. J. Kippenberg, and F. Marquardt, *Rev. Mod. Phys.* **86**, 1391 (2014).
- [S21] C. W. Gardiner and P. Zoller, *Quantum Noise: A Handbook of Markovian and Non-Markovian Quantum Stochastic Methods with Applications to Quantum Optics* (Springer-Verlag, Berlin, 2004).
- [S22] D. H. Santamore, A. C. Doherty, and M. C. Cross, *Phys. Rev. B* **70**, 144301 (2004).
- [S23] E. D. Black, *Am. J. Phys.* **69**, 79 (2001).